

Bio-robotic model as a scientific tool for experimentally investigating hydrodynamic functions of fish caudal fin

Ren Ziyu, Zhu Qichao, Wang Tianmiao, and Wen Li*

School of Mechanical Engineering and Automation, Beihang University, Beijing, 100191, People's Republic of China

Bio-robotic models become increasingly important for understanding biological system in field such as biomechanics. Fish caudal fin is a prominent example of biological propulsion, in which the caudal peduncle, fin ray and fin membrane together form a dynamic locomotory system. In this paper, we developed a bio-robotic model to mimic the fin ray structure and kinematics of Bluegill Sunfish (*Lepomis macrochirus*). We coupled controlled oscillations in both heave and pitch directions to the robot to model the caudal peduncle motion of swimming fishes. Synchronized multi-axis force transducer and particle image velocimetry were then used to quantify the hydrodynamic forces and wake flow. We found that the addition of three-dimensional fin kinematics significantly enhanced the lift force without decreasing thrust force compared with the no fin motion. The vortex wake directs water both axially and vertically and forms jet like structure with notable wake velocity. According to the bio-robotic model experimental data, we hypothesized that fish may actively control the caudal fin rays to achieve considerable lift force when swimming at low speed, however, negative at high speed.

Key words: bio-inspired robotic fish, 3D printing, caudal fin, hydrodynamics

1 Introduction

The analysis of non-traditional biomimetic propulsion swimming under controlled conditions have attracted mathematicians [1], fluid engineers [2], roboticists [3-8], material engineers [9-11] and biologists [12-16] interests in studying the principals underlying unsteady locomotion in aquatic animals. Recent advances in understanding fish caudal fin propulsion, in which oscillatory motion of a foil-like structure generate hydrodynamic forces, have included the use of robotic devices which exhibit a rich variety of dynamic behaviors similar to the fin motions of live swimming fishes [17-19]. Most previous biomimetic robotic propulsors focused on the thrust performance in the horizontal plane. The motion of robotic caudal fin has been modeled as a two-dimensional flapping (heave & pitch) as a simple extension of the undulatory body wave in most previous relevant studies [2]. The significant impact of heave & pitch motions on the hydrodynamic propulsion of foil have been investigated [20].

However, fins of most bony fishes move in three-dimensions, both caudal peduncle and fin rays move during fish these two? To our knowledge, no experimental studies have yet addressed above fish biomechanics issues, nor does any

swimming [21-23]. The peduncle motion is derived from the undulatory body wave generated by myotomal body musculature [23, 24]. While the fin rays are moved by intrinsic caudal musculature that are distinct from the body muscles. Bony fish were able to actively control both caudal peduncle motion and deform the fin surface through individually controlling the fin ray root muscle. Previous work of fish biomechanics investigated the effect of stiffness and motion program of fin rays only [25-27]. Nevertheless, no studies yet considered the peduncle motion while studying the fin locomotor functions [7, 18, 28, 29], the integrated locomotor functions by caudal fin rays and peduncle remain unexplored.

As summarized by a recent review article [30], “*bio-robotics is becoming important scientific tools and can be used to investigate locomotion and to test hypothesis*”. How do the kinematics of the peduncle and the fin rays together determine the locomotor performance of a caudal fin? How does the flow speed affect the locomotor forces and the wake flow generated by the caudal fin? Can we use a robotic experimental device to mimic both the caudal peduncle and fin ray motions and is there an optimal phase relationship between existing robotic system could allow such questions to be investigated

In this paper, we described a scientific tool for investigating hydrodynamics function of the caudal fin that mimic key

*Corresponding author (email: liwen@buaa.edu.cn)

relevant features of fish kinematic functions, therefore to investigate the hydrodynamics of caudal fin locomotion. We first designed and fabricated a robot to mimic the fin rays of Bluegill Sunfish (*Lepomis macrochirus*), and programmed it with motions that match the biological counterpart. A heave and pitch robotic system was then implemented on the towing system, which allow coupling the fish caudal peduncle motion to the fin motions and move the robot in axial direction under controlled speeds. We also simultaneously measured forces, torques and kinematics of the robot at varied

flow speeds. Wake flow analysis were conducted in both the horizontal (XY) and vertical (YZ) planes to provided two separate measurements of caudal fin from orthogonal laser light-sheet orientations. Finally, we discussed the use of bio-robotics as a scientific tool for investigating hydrodynamics function of fishes, and addressed the biological relevance of current experimental results as well as formulating several predictions and hypothesis in fish biomechanics.

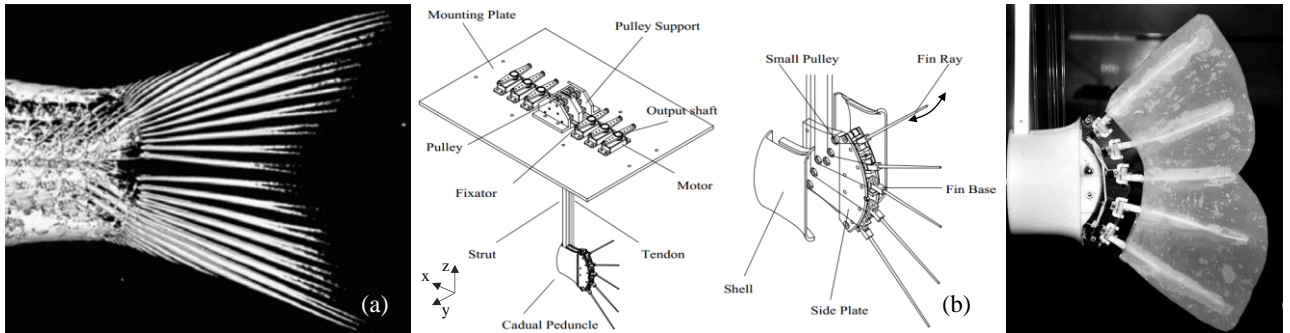


Figure 1 (a) Computer Tomography of Bluegill Sunfish caudal peduncle and fin rays [25], (b) Robotic fin demonstration in Solidworks; (c) Snapshot of the robotic caudal fin.

2 Materials and methods

A. Bio-robotic caudal fin

The mechanical design of the robotic caudal fin was based on caudal fin anatomical study of the Bluegill Sunfish [18, 23, 25] (*Lepomis macrochirus*), as can be seen from Figure 1a. For simplification, five articulated fin rays were designed to actuate the robotic caudal fin. In order to generate controlled movement patterns of fin rays, each ray was individually actuated by a servo motor (MG995, HuiSheng Inc., China) via nylon tendons with diameter of 0.6mm that was attached to each side of the fin base. Two fixators were mounted on each output shaft, which can be used for adjusting the preload force of the tendons. Tendons from the output shaft of the servo motors went along the vertical strut which is connected with caudal peduncle through group of idle pulleys, and eventually actuate the fin ray to move side-to-side. A peduncle shaped shell covered both tendons and pulleys, which also makes the flow around the caudal peduncle similar to that of a live fish (Figure 1b). Fin rays were fabricated with polylactic acid by using a 3D printer (Makerbot replicator2, MakerBot Inc., NY, USA). Robotic fin membrane is made of silicone material with thickness of 0.3mm. Silicone adhesive mixed properly with painting thinner was applied to paste silicone membranes on both sides of fin rays. A snapshot of the real robotic caudal fin is provide in Figure 1c. The quantitative data of material properties of both biological and robotic fin rays and fin membrane were provided in Table 1. It should

be note that the Young's modulus of biological and robotic fin rays are in the same order, therefore the mechanical property of the robotic fin is biologically relevant to that of a live fish.

The fin ray base was designed to actively move side to side, and have passive compliance along the folding direction. The servo motors were controlled by PWM (pulse-width-manipulated) signal individually from a microcontroller STM32F103ZET6 (STMicroelectronics Inc., EU) for controlling angular position of each fin ray movements. For each experimental trial, motion data were programmed into the controller. The controller and a DAQ card (PCI-6284, National Instrument Inc., USA) that was used for data acquisition were synchronized by a trigger signal.

B. Kinetic model of caudal fin and peduncle

To our knowledge, no previous study considered peduncle motion while studying the fin motion. There are several caudal fin movement patterns been observed, such as flat, cupping, W, rolling and undulation [25]. The biological fin motion data were digitalized in three dimensions according to high-speed videos of live fish steady swimming [26]. Among all observed caudal fin motions, rolling and undulation are particularly interested as they were hypothesized to generate superior propulsive force than other patterns according to estimation of wake flow from DPIV. To model these two motions (rolling and undulation), a reference frame was settled on vertical plane, with the origin on the tip of the lowest ventral fin ray (as shown in Figure 1b). Referring to the method used in previous study [33, 34], the mathematical

control model of rolling and undulation of the caudal fin trailing edges can be expressed as follows:

$$y_r(z, t) = \frac{a_r z}{l} \sin(2\pi f t) \quad (1)$$

$$y_u(z, t) = a_u \sin(2\pi f t + z/\lambda f) \quad (2)$$

where y_r and y_u are the horizontal displacement of the fin ray tip for rolling and undulation patterns, respectively. z denotes the vertical coordinate of the fin ray tip, t denotes the time. a_r and a_u indicate the amplitudes of the fin ray tip in rolling and undulation pattern, respectively. l is the chord length of the caudal fin, f is the motion frequency and λ is the undulation wavelength. The rotation angle of the fin base (see Figure 1b) can be derived from:

$$\vartheta_i(t) = \arcsin(y_i(t)/r_i) \quad (3)$$

where ϑ_i is the rotation angel of the i th fin base, and r_i is the length of the i th fin ray. y_i denotes the horizontal displacement of the i th fin ray which is derived from (1) or (2), depending on the motion patterns. According to the design of the mechanism of the robotic fin, the rotation angle of the server motor is proportion to that of the fin base. The caudal peduncle motion of live fish can be resolved into heave and pitch motions and can be expressed follows:

$$y_h(t) = h \sin(2\pi f t) \quad (4)$$

$$y_p(t) = p \sin(2\pi f t + 90^\circ) \quad (5)$$

where y_h denotes the caudal peduncle displacement on horizontal plane and y_p denotes the rotated angle around the vertical axis. h indicates the heave amplitude, and p indicates the pitch amplitude. In this paper, the phase difference between heave and pitch motions was set to 90° for all experimental trials.

Table 1 Shape and mechanical characterization parameters of the robotic caudal fin and the biological fin [25]

Variable	Value
Span length (mm)	183
Chord length (mm)	160
Young's modulus of robotic fin ray (Nm^{-2})	4.9×10^9
Young's modulus of biological fin ray (Nm^{-2})	$10^8 \sim 10^9$
Fin membrane thickness (mm)	0.6
Elongation rate of robotic fin membrane	300%

C. Hydrodynamic characterization

Figure 2a shows the schematic view of the experimental apparatus for the hydrodynamic characterization. The water tank has a dimension of 7.8m in length, 1.2m in width and 1.1m in height. A guide rail that was actuated by a 4000 watt AC motor with a travel distance of 7.5m, a position accuracy

of 0.1mm and a maximum speed of 3m/s set vertically above the water tank. A servo towing system was used to generate precisely controlled towing speed. A carriage assembled with the guide rail integrated capabilities of both translational and rotational movements. The translational and rotational motions were actuated by servomotors and were used for generating heave and pitch motions for bio-robotic caudal fin model. The robotic caudal fin was designed to move at mid-depth of the water tank to avoid the interference effect of the free surface and the bottom of the tank. More details of the towing system and water tank can refer to our previous work [3, 5, 31].

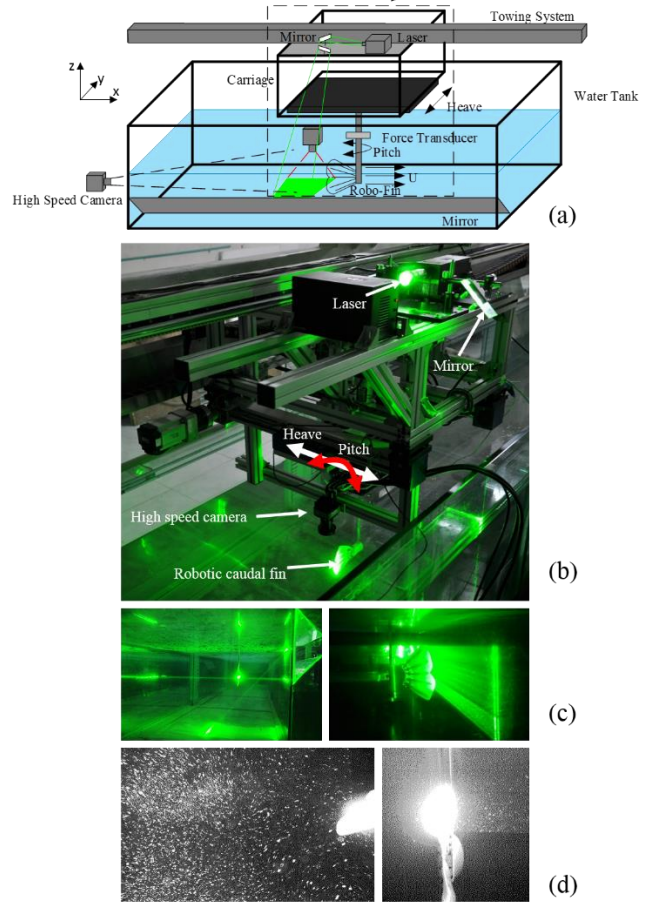


Figure 2. (a) Schematic view of the experimental apparatus; (b) Snapshot of experimental apparatus with laser system in operation; (c) Snapshots of caudal fin with laser planes across mid-plane and vertical plane; (d) High speed camera image of the illuminated particles in horizontal and vertical views.

To measure the hydrodynamic forces generated by the robotic caudal fin, a multi-axis force transducer (mini-40, ATI Industrial Inc., Canada) assembled with the heave & pitch robotic carriage connected the bio-robotic caudal fin model. The force transducer allows three forces and three torques to be measured simultaneously. The force data were then collected by the DAQ card (PCI-6284, National Instru-

ment Inc., USA). As shown in Figure 2b, the high speed camera shown was used to record the images of particles movement in water. Flow was visualized by seeding the water with near-neutrally buoyant glass beads $10\mu\text{m}$ in diameter which reflected light from a 4W laser with wavelength of 532nm. Laser sheets were projected horizontally in water by several mirrors. The horizontal laser sheet was around 1mm thick and 150mm wide and was positioned at the mid-sagittal plane of the caudal fin. The vertical laser sheet was approximately 1mm thick and 100mm wide. Figure 2c shows snapshots of particles in both horizontal and vertical planes. Particle images of both vertical and horizontal were recorded with high speed cameras at frequency of 125Hz. Particle images by high speed camera in horizontal and vertical plane can be seen in Figure 2d. The whole experimental system was controlled by a Labview program (National Instrument Inc., USA). The motion of the bio-robotic caudal fin, the force data and the high speed particle images can be simultaneously recorded by a trigger from the Labview program.

3 Results

A. Kinematics

Systematic tests were performed for the robotic caudal fin hydrodynamics at fixed heave and pitch motion amplitude and frequency. The heave motion was conducted at $f=1\text{Hz}$, $h=2.5\text{Hz}$, while the pitch motion was set to $f=1\text{Hz}$, $\theta=10^\circ$. By controlling the towing system, caudal fin hydrodynamic force measurements were conducted at three different towing speeds: $U=0\text{cm/s}$, 5cm/s and 10cm/s . For caudal fin ray movements, the frequency was set to 1Hz which is consistent with the frequency of the peduncle motion. All these motion parameters were selected as they are biological relevant to real fish swimming kinematics. Figure 3a shows the snapshot of the undulation motion (coupling with heave & pitch) of the robotic fin model at one instant. Figure 3b~3d show the trailing edge trajectories of three fin movement patterns during one flapping cycle. The trailing edge trajectories under different movement patterns were extracted from the high speed videos using a self-developed Matlab program. Three movement patterns were investigated in this paper: 1) no fin motion (Figure 3b), in which all fin rays were held still without angular movements through a tail beat cycle; 2) undulation pattern (Figure 3c) with wavelength of 160mm, amplitude of 20mm; 3) rolling pattern (Figure 3d) with maximum amplitude of 20mm and minimum amplitude of 10mm. To investigate the effect of phase angle between movements of the caudal peduncle and the fin rays on the hydrodynamic force of the bio-robotic caudal fin, the phase angle was systematically investigated from 0° to 315° with increment of 45° while keeping the rest motion parameters under undulation mode constant under towing speed of 0cm/s .

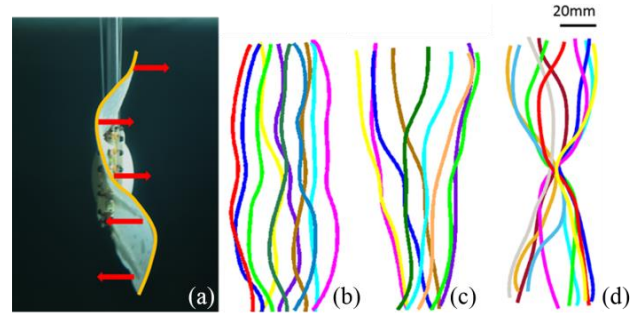


Figure. 3. (a) Snapshot of dynamic moving caudal fin from the high speed camera, the yellow curve indicates the trailing edge of the caudal fin; and the red arrows indicate direction of individual fin ray movement. At $U=0\text{cm/s}$, trailing edge trajectories of caudal fin under (b) no fin motion, (c) rolling, and (d) undulation are demonstrated.

B. Hydrodynamic force

We first investigate the mean thrust force and mean lift force (force averaged from one flapping cycle) generated by three different movement patterns under different towing speeds. All these tests were performed with phase angle of 0° . Data of mean thrust force and mean lift force are shown in Figure 4a and 4b. It can be observed that mean thrust force and lift force of bio-robotic caudal fin varied with towing speed U . For all three movement patterns, i.e., no fin motion, rolling and undulation, mean thrust force decrease as U increases. This can be considered as a directly consequence as the drag force increased due to an increasing towing speed. At $U=0\text{cm/s}$, no fin motion pattern generated the maximum mean thrust force, with a force magnitude of $0.063\pm 0.001\text{N}$, 5% greater than the undulation pattern, and significantly larger than the rolling pattern by 26%. As the towing speed increased to $U=5\text{cm/s}$, however, the mean thrust force produced by undulation motion with a magnitude of $0.008\pm 0.003\text{N}$ exceeded the other two motions, while the thrust magnitude of no fin motion and rolling were almost zero. As $U=10\text{cm/s}$, the mean thrust force became negative, which in turn indicate that the thrust force generated by the caudal fin was insufficient to overcome the drag force. The mean thrust force of three motion under this condition were $-0.026\pm 0.002\text{N}$, $-0.027\pm 0.004\text{N}$ and $-0.010\pm 0.001\text{N}$. The undulation again produced maximum mean thrust force that were around 60% larger than those of no fin motion and rolling. It is noteworthy that, the mean lift force of rolling and undulation decreased significantly as the towing speed increased. The rolling motion produced mean lift force of $0.050\pm 0.006\text{N}$ under $U=0\text{cm/s}$, which was significantly greater than those produced under 5cm/s and 10cm/s . The undulation motion generated mean lift force of $0.055\pm 0.009\text{N}$ under $U=0\text{cm/s}$, which was 17% and 400% larger than those under 5cm/s and 10cm/s . From aspect of average force, the mean lift forces generated by undulation were larger than those of the rolling under 0cm/s and 5cm/s . However, when flow speed increased to 10cm/s , the magnitude of the lift

force generated by rolling movement surpassed that of undulation. In particular, the no fin motion generates very small mean lift force at all flow speeds which was consistent with the experimental data by Esposito et al. [25] and the theoretical work conducted by Affleck et al. [32]

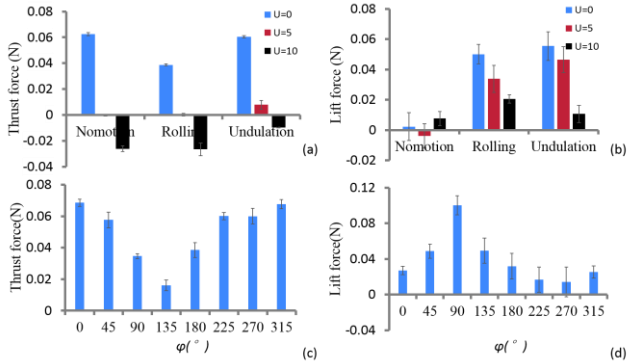


Figure 4. Mean thrust (a) and lift force (b) under $U=0, 5$ and 10cm/s for three fin movement patterns: no fin motion, rolling and undulation. Thrust force (c) and lift force (d) as function of phase difference ($\phi=0^\circ\sim 315^\circ$) between caudal peduncle and fin ray motion were tested.

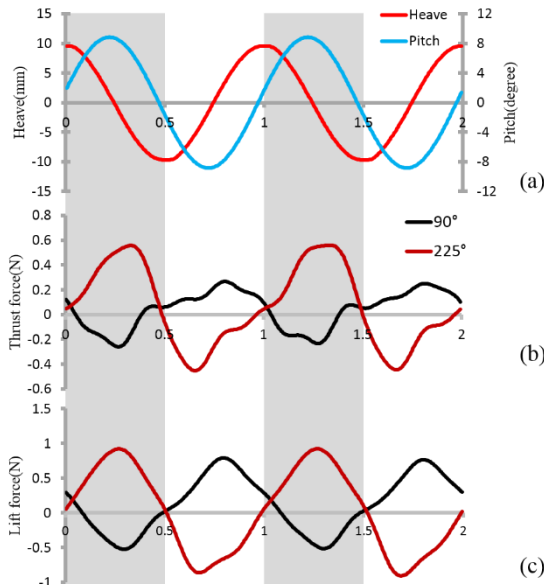


Figure 5. Instantaneous force for two caudal fin motion cycles; (a) heave and pitch motions for two motion cycles; (b) thrust force at $\phi=90^\circ$ and 225° ; (c) lift force comparison at $\phi=90^\circ$ and 225° .

The force data from experimental groups with different phase angle were summarized in Figure 4c and 4d. Pronounced periodical trend can be observed. The mean thrust force reached its maximum value at $\phi=0^\circ$ and decreased as the phase angle increased until 135° , at which the thrust force reached a minimal peak with magnitude of $0.016\pm 0.003\text{N}$. The peak-to-valley ratio was about 4.5. While mean lift force increased with phase difference until 90° , at which the mean lift force reached a maximum peak with magnitude of $0.100\pm 0.01\text{N}$, and then decreased until the phase angle reached 270° . The peak-to-valley ratio was about 8.0.

Instantaneous force during two flapping cycles at $\phi=90^\circ$ and $\phi=225^\circ$ were shown in Figure 5, under which maximum and minimal mean lift force were generated among all phase tests. The forces are significantly different in terms of both profile and magnitude. Pitch motion seemed to play a leading role in affecting instantaneous force. When phase angle was 90° , thrust force gradually decrease as pitch motion reached its maximum velocity, which was when it passed through the mid-position (Figure 5a). As the pitch motion reversed direction, the thrust force gradually increased from a minimum negative value. When pitch motion again reached its maximum velocity, the thrust force almost became zero. With the pitch motion from the mid-point to the other side of the extreme lateral position, the thrust force continued increased. But before the maximum peak thrust force, the profile always became flattened. Similar experimental results could be found in previous literature. The trend of lift force profile was almost the same with the thrust force besides this phenomenon. As for $\phi=225^\circ$, the trend of force profile was nearly reversed. The maximum force at $\phi=225^\circ$ always occurred around the time when minimum force reached at $\phi=90^\circ$, and minimum force at $\phi=225^\circ$. In addition, no apparent “flattened” phenomenon was observed.

C. Wake flow

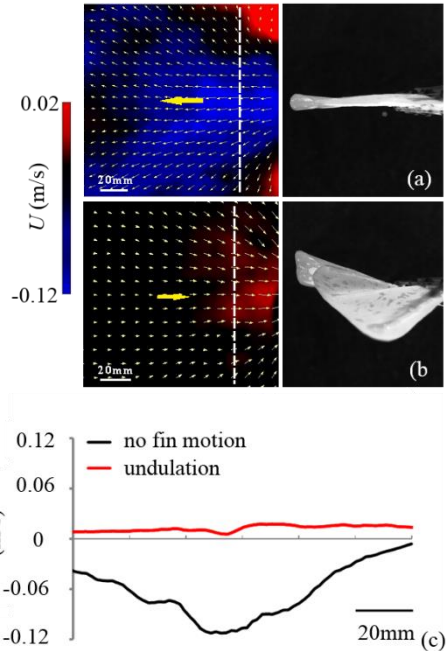


Figure 6. Average speed in the horizontal plane based on the particle image velocimetry analysis; (a) no fin motion Horizontal; (b) fin undulation at $\phi=90^\circ$; (c) average horizontal jet velocity in U direction.

We conducted particle image velocimetry (PIV) measurements on the caudal fin with the no fin motion and undulation pattern from both horizontal and vertical planes under zero towing speed ($U=0$). The average wake jet velocities on

horizontal and vertical planes are provided in Figure 6 and 7. In Figure 6, the average wake flows on horizontal plane were totally different between two patterns. For no fin motion, caudal fin “push” the flow downstream (Figure 6a) with a relatively large speed, in contrast the magnitude of wake flow speed of undulation pattern was relatively small. The result even indicates that the flow was “suck” forward towards upstream (Figure 6b). For a further comparison, we chose to compare average wake velocity on the horizontal in U direction which we marked in Figure 6a and 6b with a white dotted line. The average wake velocity profiles of the two motions are shown in Figure 6c. In the horizontal plane, jet speed of undulation along the white line is close to zero, while the control motion generates significant jet flow speed with a peak at around middle position of an entire stroke (Figure 6c).

On vertical plane, we recorded the wake flow of the upper lobe of the fin only (as the laser plane covers the upper part of the fin only). The jet flow direction of no fin motion pattern was downward (Figure 7a), which has opposite direction compared with the flow generated by the undulation pattern (Figure 7b). This phenomenon is also clearly reflected by jet velocity, as can be seen from figure 7c.

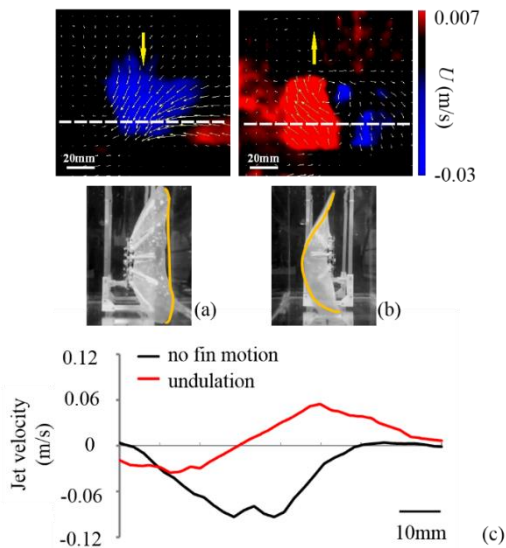


Figure 7. Average speed in the vertical plane based on the particle image velocimetry analysis; (a) no fin motion Horizontal; (b) fin undulation at $\phi=90^\circ$; (c) average vertical jet velocity in U direction.

4. Discussion and Conclusion

Bio-robotics could become part of the scientific process of making progress and new hypothesis while studying the fish biomechanics [30]. Measuring forces and flow from freely swimming live fishes is always challenging [13]. Although

there were some previous functional locomotor studies of biological caudal fin, the inability to manipulate and isolate key biomechanical parameters has hindered our understanding of caudal fin propulsion, for example, the hydrodynamic effect of caudal peduncle, the fin ray movement patterns and the swimming speed. The bio-robotic model described in this paper was proven to have capabilities of generating kinematics matching that of freely-swimming fishes. The current experimental apparatus allows for collecting useful scientific data of fish biomechanics, such as XYZ forces and wake flow in both horizontal and vertical planes, under controlled flow speeds. We summed up current experimental results and formulated several new predictions:

(i) The addition of heave and pitch motions of caudal peduncle were not taken into account by predecessors [23, 25, 26], which have significant impact on the hydrodynamic performance of overall caudal fin propulsion.

(ii) The lift force decrease dramatically as flow speed increase. Therefore, we hypothesises that fish may actively change their fin locomotor shapes to achieve considerable lift force at low swimming speed. At higher swimming speed, however, three-dimensional fin motions were not able to generate significant lift force.

(iii) Using the no fin motion as a control, robotic fins with undulation motion generate significantly larger lift forces. In addition, the time-averaged wake jets in both horizontal and vertical planes are notably different from that of no fin motion. Altering the fin ray motion, caudal peduncle motion, or the phase difference between these two would result in significant different thrust and lift forces.

The addition of a mechanism that generates controlled caudal peduncle-like flapping motion to a robotic fin ray system provides a new experimental avenue for studying the hydrodynamics of fish caudal fin, as well as other bio-robotic model with three-dimensional locomotion. Besides understanding fundamental questions in biomechanics of fish swimming, the design and experimental results may also be leverage to future non-traditional propellers [20]. The experiments described here focused on swimming of caudal fin in steady swimming state, but of equal interest is hydrodynamics of caudal fin during non-steady-state, for example, acceleration, deceleration and turning etc. Future work will include more systematic parametric studies of the caudal fin kinematics and conduct experiments under non-steady-state conditions.

A. Effect of flow speed

Testing hydrodynamic performance of caudal fin movement

patterns under different flow speeds would be helpful for answering two important questions: 1) how the flow speed affect the forces produced by the caudal fin movement and 2) which is the optimal movement pattern of caudal fin under a given flow speed. According to current experimental results, increasing towing speed remarkably decrease the lift force both in undulation motion and rolling motions. One possible explanation may locates on the fact that, both rolling and undulation motion patterns produce jet flow in the vertical plane. The oncoming water flow speed to the caudal fin increased as fish swimming speed, while accelerated water flow speed may decrease the angle between jet flow and horizontal plane, therefore result in decrease of lift force. We also found that, when fish swims under high speed, the three-dimensional fin motions has little hydrodynamic functions on the maneuverable force in vertical plane. In contrast, when fish hovers or swims under a relatively low speed, the caudal fin movement may play a critical role in generating lift force, and therefore provide considerable pitch maneuvering. In fact, for many high swimming speed fishes like tuna, the caudal fin is relatively stiff and is not able to generate complex three-dimensional motion pattern. Three-dimensional caudal fin ray locomotion have been observed in many bony fishes such as bluegill under low swimming speed, however, rarely been reported at high steady swimming speed [26].

B. Effect of adding peduncle motion

The motion of the fish caudal fin rays is always coupled with the motion of peduncle. Although the caudal fin peduncle motion have be commonly treated as a “trailing edge” of the fish body undulation, the overall hydrodynamic performance of the caudal fin rays and the caudal peduncle remain unexplored. Additional heave and pitch motion can significantly change the kinematics of the fin rays, such as the amplitude, trailing edge trajectories, etc. Besides, different phase angle between caudal peduncle motion and fin ray motion have significant impact on lift and thrust force. We found that the lift force reached the maximum peak value at $\varphi=90^\circ$, however, very small thrust force was generated; but for other case (i.e., $\varphi=270^\circ$), the thrust force was large, while rather small amount of lift force was generated. When fish hovering under still flow condition, considerable lift force could be produced while generating little thrust force (these additional thrust can be balanced by other fins such as pectoral fins). When the fish chases a prey in the vertical plane, both significant thrust and lift force are required, the addition of phase angle at $\varphi=45^\circ$ between the caudal peduncle and fin rays would be quite beneficial. Based on current experimental data, we predict that real fish may actively modulate the phase angle between the caudal peduncle motion and the fin ray motion for different behaviors, such as prey, escape and migration.

Many thanks to Cai Yingjie, Wang Yueping and Wang Zaijun for their help in implementing the experimental apparatus and programming motion

of the robotic fin. This work was supported by the National Science Foundation support projects, China under contract number 61403012 (to Li Wen), Beijing Science Foundation support projects under contract number 4154077 (to Li Wen) and National Science Foundation support projects, China under contract number 61333016 (to Tan Min).

- 1 Alben S, Witt C, Baker T V, et al. Dynamics of freely swimming flexible foils. *Phys. Fluids* (1994-present), 2012, 24(5): 051901.
- 2 Anderson J M, Streitlien K, Barrett D S, et al. Oscillating foils of high propulsive efficiency. *J. Fluid Mech.*, 1998, 360: 41-72.
- 3 Wen L, Wang T, Wu G, and Liang J H. Hydrodynamic investigation of a self-propulsive robotic fish based on a force-feedback control method. *Bioinspir Biomim*, 2012, 7: 036012.
- 4 Wen L, Weaver J C, Lauder G V. Biomimetic shark skin: design, fabrication and hydrodynamic function. *J Exp Biol*, 2014, 217(10): 1656-1666.
- 5 Wen L, Wang T, Wu G, et al. Quantitative thrust efficiency of a self-propulsive robotic fish: experimental method and hydrodynamic investigation. *Mechatronics, IEEE/ASME Transactions on*, 2013, 18(3): 1027-1038.
- 6 Yun D, Kim K S, Kim S, et al. Actuation of a robotic fish caudal fin for low reaction torque. *Rev Sci Instrum*, 2011, 82(7): 075114.
- 7 Low K H, Chong C W. Parametric study of the swimming performance of a fish robot propelled by a flexible caudal fin. *Bioinspir Biomim*, 2010, 5(4): 046002.
- 8 Zhou C, Chao Z Q, Wang S, et al. A marsupial robotic fish team: Design, motion and cooperation. *Sci China Tech Sci*, 2010, 53: 2896-2904.
- 9 Wang Z, Hang G, Wang Y, et al. Embedded SMA wire actuated biomimetic fin: a module for biomimetic underwater propulsion. *Smart Mater Struct*, 2008, 17(2): 025039.
- 10 Shen Q, Wang T, Liang J, et al. Hydrodynamic performance of a biomimetic robotic swimmer actuated by ionic polymer-metal composite. *Smart Mater Struct*, 2013, 22(7): 075035.
- 11 T M Wang, Q Shen, Li Wen, J H Liang “On the thrust performance of an ionic polymer-metal composite actuated robotic fish: modeling and experimental investigation”. *Sci China Tech Sci*, 2012, 55(12): 3359-3369.
- 12 Barrett D S, Triantafyllou M S, Yue D K P, et al. Drag reduction in fish-like locomotion. *J. Fluid Mech*, 1999, 392: 183-212.
- 13 Lauder G V. Swimming hydrodynamics: ten questions and the technical approaches needed to resolve them. *Animal Locomotion*. Springer Berlin Heidelberg, 2010: 3-15.
- 14 Wu G H, Yang Y, and Zeng L J. Kinematics, hydrodynamics and energetic advantages of burst-and-coast swimming of koi carps (*Cyprinus carpio koi*). *J Exp Biol*, 2007, 210: 2181-2191.
- 15 Wu G H, Yang Y, and Zeng L J. Novel method based on video tracking system for simultaneous measurement of kinematics and flow in the wake of a freely swimming fish. *Rev Sci Instrum*, 2006, 77: 114302.
- 16 Arash T, Sakineh O. A novel miniature virus-inspired swimming robot for biomedical applications. *Sci China Tech Sci*, 2010, 53:2883-2895.
- 17 Oeffner J, Lauder G V. The hydrodynamic function of shark skin and two biomimetic applications. *J Exp Biol*, 2012, 215(5): 785-795.
- 18 Lauder G V, Flammang B, Alben S. Passive robotic models of propulsion by the bodies and caudal fins of fish. *Integr Comp Biol*, 2012: ics096.
- 19 Wen L, Lauder G V. Understanding undulatory locomotion in fishes using an inertia-compensated flapping foil robotic device. *Integr Comp Biol*, 2012, 52: 189.
- 20 Triantafyllou M S, Triantafyllou G S. An efficient swimming machine. *Sci Am*, 1995, 272(3): 64-71.
- 21 Lauder G V, Drucker E G, Nauen J, et al. Experimental hydrodynamics and evolution: caudal fin locomotion in fishes. *Vertebrate biomechanics and evolution*, 2003: 117-135.
- 22 Nauen J C, Lauder G V. Hydrodynamics of caudal fin locomotion by chub mackerel, *Scomber japonicus* (Scombridae). *J Exp Biol*, 2002, 205(12): 1709-1724.

- 23 Flammang B E, Lauder G V. Speed-dependent intrinsic caudal fin muscle recruitment during steady swimming in bluegill sunfish, *Lepomis macrochirus*. *J Exp Biol*, 2008, 211(4): 587-598.
- 24 Wilga C D, Lauder G V. Function of the heterocercal tail in sharks: quantitative wake dynamics during steady horizontal swimming and vertical maneuvering. *J Exp Biol*, 2002, 205(16): 2365-2374.
- 25 Esposito C J, Tangorra J L, Flammang B E, et al. A robotic fish caudal fin: effects of stiffness and motor program on locomotor performance. *J Exp Biol*, 2012, 215(1): 56-67.
- 26 Flammang B E, Lauder G V. Caudal fin shape modulation and control during acceleration, braking and backing maneuvers in bluegill sunfish, *Lepomis macrochirus*. *J Exp Biol*, 2009, 212(2): 277-286.
- 27 Lauder G V, Lim J, Shelton R, et al. Robotic models for studying undulatory locomotion in fishes. *Mar Technol Soc J*, 2011, 45(4): 41-55.
- 28 Curet O M, Patankar N A, Lauder G V, et al. Mechanical properties of a bio-inspired robotic knifefish with an undulatory propulsors. *Bioinspir Biomim*, 2011, 6(2): 026004.
- 29 Curet O M, Patankar N A, Lauder G V, et al. Aquatic manoeuvring with counter-propagating waves: a novel locomotive strategy. *J R Soc Interface*, 2010: rsif20100493.
- 30 Ijspeert A J. Biorobotics: Using robots to emulate and investigate agile locomotion. *Sci*, 2014, 346(6206): 196-203.
- 31 Li Wen, T M Wang, G H Wu and J H Liang, "Hybrid Undulatory Kinematics of a Robotic Mackerel (*Scomber scombrus*): Theoretical Modeling and Experimental Investigation". *Sci China Technol Sc*, 55 (10): 2941-2952, 2012.
- 32 Affleck R J. Some points in the function, development and evolution of the tail in fishes. *Proceedings of the Zoological Society of London*. Blackwell Publishing Ltd, 1950, 120(2): 349-368.
- 33 Zhou H, Hu T J, Xie H B, et al. Computational and experimental study on dynamic behavior of underwater robots propelled by bionic undulating fins. *Sci China Tech Sci*, 2010, 53: 2966-2971.
- 34 Wang G, Zhang D B, Lin L X, et al. CPGs control method using a new oscillator in robotic fish. *Sci China Tech Sci*, 2010, 53: 2914-2919.